Protection and Control Challenges of Low-Voltage Networks with High Distributed Energy Resources Penetration — Part 1: Utility Workshop and Low-Voltage Network Modeling

Zheyuan Cheng, Eric Udren, Juergen Holbach
Quanta Technology
Raleigh, NC, USA
{zcheng, eudren, jholbach}@quanta-technology.com

Matthew J. Reno, Michael E. Ropp
Sandia National Laboratories
Albuquerque, NM, USA
{mjreno, meropp}@sandia.gov

***Abstract*—The growing distributed energy resources (DER) penetration in the low-voltage network (600V and below) challenges the existing protection philosophy and practice. To assess the impact of high DER penetration, the authors built a representative low-voltage network model in real-time electromagnetic transient software and performed hardware-in-the-loop (HIL) protection studies. In the first stage of the effort, the authors invited four major U.S. utilities with low-voltage networks to a technical workshop to survey the modeling and study needs. Guided by the workshop discussions, the authors developed various real-time simulation models, including a low-voltage network model, a model of a commonly used network protector relay, and DER models. Finally, the authors conducted hardware-in-the-loop protection studies to investigate and mitigate the high DER penetration impacts. Part 1 of the paper summarizes the technical workshop outcomes and low-voltage network modeling approaches. Part 2 of the paper reports the HIL simulation setup, high DER penetration impact assessment, and benchmark results of a promising mitigation solution.**

***Index Terms*—Distributed Energy Resources, Hardware-in-the-loop Simulation, Low-voltage Networks, Protective Relaying, Real-Time Digital Simulation.**

I. Introduction

As its name suggests, low-voltage networks operate at a low voltage level, e.g., 120/208V and 207/480V. They are also referred to as secondary networks in some literature. Typically, they are categorized into two types: spot networks and grid networks. A spot network is a small network, usually at one location, consisting of two or more primary feeders with network units. A grid network is typically highly meshed and supplied by numerous network units. Both networks are widely used for serving concentrated loads in dense urban areas. The reliability of low-voltage networks is critical, as interruptions can black out major load centers and have serious safety and public-impact consequences.

Increasingly, customers are connecting distributed energy resources (DER) to the low-voltage network. Additional DER generation can offset the demand peak and even back-feed the primary feeder. Moreover, most newly added DER are inverter-based resources (IBR), e.g., solar and battery, with anomalous behaviors during faults and disturbances. Current low-voltage network protection systems are designed to clear faults on the primary feeder by detecting excessive reverse current (or power). The combination of DER back-feed and IBR anomalous fault response poses a significant challenge to the existing low-voltage network protection philosophy and practice. It is worth noting that the impact of high DER penetration does not limit to protection. It also poses a bundle of challenges to low-voltage network operation. A more holistic view of the DER challenges in the low-voltage network can be found in [1]. As far as this paper is concerned, the research focus is placed on the challenges related to protection and control.

In anticipation of making research findings and data available to the public, authors intentionally steered away from modeling a real-world low-voltage network with proprietary data. We tried to identify a representative open-source benchmark system to perform protection studies. According to [2], only three test feeders contain low-voltage networks: (1) IEEE 8500-node system, (2) European low-voltage test feeder, (3) non-synthetic low-voltage European test network, (4) IEEE low-voltage network test system (LVNTS). The IEEE 8500-node system is a large 12.47kV radial distribution system that includes spot networks (120V-240V) via split-phase service transformers. Although it contains some spot networks, this model is not well-positioned for low-voltage grid network studies. Similar to the IEEE 8500-node system, the two European test systems are radial systems that do not capture the characteristics of low-voltage grid networks. The European low-voltage test feeder is an underground cable low-voltage (416V at 50Hz) radial distribution network serving a residential area. The non-synthetic low-voltage European test network has 30 substations with 10290 buses and 8087 loads [3]. This European 4-wire system is also largely a radial suburban distribution network. IEEE LVNTS is a heavily meshed underground cable low-voltage (120/208V) grid network serving a dense urban area. Moreover, it also includes numerous 207/480V spot low-voltage networks. IEEE LVNTS contains lots of parallel

network transformers and primary feeders [4]. Overall, the IEEE LVNTS is the best candidate for the purpose of this paper. At the time being, open-source and pre-built models of IEEE LVNTS can only be found in GridLAB-D and OpenDSS. But neither of them supports the time-domain electromagnetic transient (EMT) study. Therefore, the IEEE LVNTS was modeled from scratch in the RSCAD/RTDS.

The authors of this paper have investigated the impact of DER in low-voltage networks in two prior works published in [5] and [6]. According to our literature review, most DER-related research efforts have been oriented toward distribution systems and microgrid applications. The high DER penetration impact on low-voltage grid networks, especially the impact on network protection, is less understood. One of the early DER-related studies in low-voltage grid networks is published in [7]. The low-voltage grid network selected for this study supplies part of the Manhattan area. It has 12 primary feeders, 224 transformers, 224 network protections, and 311 aggregated loads. The EMTP simulation software is used to study DER hosting capacity. In [8], a part of the low-voltage grid network in the city of New Orleans is modeled as a balanced three-phase system, and the authors conducted steady-state power flow studies to analyze DER impacts on network protection. In [9], a Brazilian 81-bus test system and the IEEE LVNTS are simulated in OpenDSS to study the impact of DER reverse power flow on network protection. With respect to prior works, the key contributions of this Part 1 paper are summarized as the following: (1) This paper reports low-voltage network protection challenges the industry faces today. (2) A large-scale and low-voltage grid network is modeled and benchmarked in a real-time EMT simulator.

The rest of the paper is structured as follows: Section II reports the challenges utilities face today and the new technologies they have been exploring. Section III presents the modeling approach of a low-voltage network and benchmark analysis. The conclusions are summarized in Section IV.

II. Utility Technical Workshop

Utility subject matter experts from Consolidated Edison Company of New York (ConEd), Commonwealth Edison Company, Oncor Energy Delivery, and PEPCO/PHI, are invited to participate in a half-day workshop to discuss their current low-voltage network protection situations, challenges, and future research needs. The discussions were summarized as four major challenges as the following. More details of the workshop discussion can be found in [10].

A. DER Backfeed Induced NP Misoperation

One of the most frequently visited topics in the workshop is the DER backfeed. Participated utilities all reported growing integration of DERs, e.g., PEPCO's recent renewable DER integration target is 10%. As more DER are added to the low-voltage network, the added generation could offset the demand peak and even back-feed to the primary feeder or main service. The low-voltage network with DER reverse power flow is one of the most challenging operating scenarios reported by the utility participants. Some current challenges reported by utility participants are:

- Having trouble allowing more DER reverse power flow without protection misoperation.
- Cannot reliably distinguish DER back-feed and primary feeder faults.
- Need for a better DER management system to operate and monitor a large number of DERs.
- The need to leverage DER to reduce peak demands and avoid curtailment.
- It is challenging to increase the DER hosting capacity of the low-voltage network without impacting the protection and reliability.

Two novel protection practices are reported by the ConEd to avoid protection misoperations during DER reverse power flow:

- Rate-of-change based detection: use rate of change settings to distinguish slow changes in current during back-feed (rapid change is the fault).
- Substation transfer trip: Install transfer trip capability on network protectors; configure network protectors in an extremely insensitive mode; and let the substation relay transfer trip network protectors.

According to ConEd's experience, the first rate-of-change method is not perfect, as it may have gaps and may misoperate for external transmission faults. Additionally, setting the rate-of-change threshold can be a case-by-case task for different low-voltage networks. Although these two practices are currently used in ConEd's system, neither is optimum.

An interesting observation on DER in distribution is reported by ConEd. Currently, the low voltage networks with high DER-to-load ratios are usually spot networks. The grid networks, e.g., those in New York City, have less DER penetration. However, the DER penetration in grid networks is likely to increase in 5–10 years.

B. Voltage Profile Management

Another challenge mentioned along with the DER reverse power flow is voltage regulation. Significant DER back-feed could cause serious voltage profile issues, e.g., over-voltage and fluctuation, which will, in turn, put stress on voltage regulators in the low-voltage network. Nowadays, advanced smart inverter functions, e.g., droop control, constant power, current, and voltage control modes, have become readily available due to earlier standardization efforts such as IEEE 1547-2018. If used intelligently, these newly added functionalities may provide more flexibility or even solve some of the voltage profile management problems. Some current challenges reported by utility participants are:

- DER's smart inverters, e.g., reactive power injection, could negatively impact voltage regulation. Additional coordination between DER and voltage regulators is needed.
- How to leverage inverter-based DER to improve the low voltage network voltage profile.

- Voltage profile changes over season, time, and weather. For weaker areas, it is difficult to manage the voltage profile.

As for voltage regulation practice, ConEd reported that they typically use fixed tap network transformers, whereas PEPCO uses network transformers with automatic tap changers. The control coordination between the voltage regulator and smart inverter can be circumvented if fixed-tap network transformers are used across the low-voltage network. However, the tap positions need to be determined based on the actual voltage drops in the field that typically correlate to the distance to the substations and seasonal voltage profile. An interesting observation related to voltage control is reported by ConEd. Based on their experience, conservation voltage reduction generally allows higher DER reverse power flow.

C. Slow Clearing of Secondary Cable Faults

One of the most pressing issues utilities face is the detection and fast clearing of secondary cable faults. Generally, the protection philosophy dictates the network protectors clear reverse faults and leave the low-voltage network faults to passive devices such as fuses and cable limiters. The lack of sensing devices, e.g., current transformers (CT), in the low-voltage network makes the fault location difficult, if not impossible. Additionally, the fault currents on the fuses are usually very high, and the fault is usually burned clear, which could cause smoke, fire, or even explosion hazards. Some current challenges reported by utility participants are:

- The detection and fast clearing of slowly developing cable faults is a huge problem. The signatures of this type of fault are not fully understood.
- The visibility of the secondary low-voltage network is very limited. More weatherproof sensors and monitoring tools are needed to detect and locate secondary faults.
- Need for better real-time power flow model and tools for contingency analysis during faults.

According to ConEd's experience, the common cause of the slow-developing cable faults in New York City is the corrosion associated with salt and snow melting. These fault events occur approximately 3000 times per year in New York City. To address this pressing issue, ConEd has deployed an infrared (IR) camera-based fault detection system to detect and locate hot spots caused by high loads and faults. These IR camera sensors operate on the battery and communicate to the operator via wireless communication, i.e., LTE cellular network. So far, this IR camera system has been delivering satisfactory fault detection and location performance. However, one major drawback of this IR camera sensor system is the battery replacement. Currently, approximately 50% of the IR camera sensors are not operational due to dead batteries.

Participated utilities reported similar low-voltage network CT placement practices – placing the SCADA-connected CT strategically at the major node of the low-voltage network to monitor the load current. It is also common for utilities to leverage the measurements from network transformers and advanced metering infrastructure (AMI) to monitor the load and fault currents.

In terms of low voltage fault clearing, ConEd has been deploying medium voltage interrupters to sectionalize low voltage networks. These devices provide great flexibility for fault clearing and service restoration.

As for contingency analysis, PEPCO reported that the lack of a real-time power flow model significantly limits their ability to determine the power flow quickly and accurately in the cable and lines during contingency. Having a real-time power flow tool would also help to estimate the states, e.g., load, voltage, current, etc., of the low voltage network during normal operation, thus improving the visibility. There may be a good research opportunity to develop a real-time power flow tool that uses system model data, AMI data, and field measurements.

During the discussion of secondary cable faults, PEPCO mentioned research challenges and opportunities on the topic of predictive cable faults and failure analysis. Some research work has been done to develop data-driven methods to identify cable failure signatures and precursors.

D. Microgrid Integration

As part of the low voltage network, microgrids have been frequently developed to harness DERs and provide extremely high reliability to customers. Microgrid protection by itself is a very complex and intriguing research topic. From the workshop participants' perspective, the protection within the microgrid should be treated separately in general. The coordination between the microgrid tie-breaker and low-voltage network protection is of interest to this study.

There are two types commonly seen microgrids within or connected to the current low voltage networks: (1) customer site microgrid that is connected to the low voltage network (may have multiple connection points), and (2) microgrid with significant DER that is connected to the medium voltage primary feeder. During an outage, the type-1 microgrids can disconnect from the rest of the low-voltage network and restore on-site electric service. In contrast, the type-2 microgrid can potentially feed energy via the primary feeder and restore part of or the entire low-voltage network.

E. Focus of this Paper

This paper series is dedicated to investigating the first and likely the most pressing issue that participating utilities are facing — DER reverse real/reactive power flow impacts. Other research topics are reserved for future research efforts. The ultimate test goals of this paper are:

- Evaluate the impact of DER reverse real power flow on the existing protection schemes.
- Propose and benchmark new protection solutions that allow more DER P/Q back-feed without misoperation.

III. Low-voltage Network Modeling

This section entails the modeling of individual components as well as the IEEE LVNTS in the RSCAD software. Both steady-state and short-circuit benchmarks are proposed to validate the model.

A. Component Modeling

The loads at each bus are modeled as constant power loads. There are two load types at each bus (i.e., single-phase load and phase-to-phase load). The dynamic load model in RSCAD uses the local voltage measurement as feedback to regulate power consumption. For example, the dynamic load will increase its current suction if the bus voltage decreases.

An induction motor load that can become a generator during fault conditions (e.g., a large elevator motor load) is also modeled in addition to constant power loads. The fault current injected by the induction motor will introduce additionally needed dynamics to the constant power load dynamics. The motor load is modeled as a three-phase induction motor using RTDS native induction motor module. This motor is assumed to be connected to the 480V spot network via a 13.8kV–480V delta–Wye network transformer.

The inverter-based DER model used in this study is a detailed switching model of a 208/120V neutral-point-clamped (NPC) inverter that is developed based on a proprietary vendor inverter-based DER model. A scaling factor is applied to this DER so that it can be used to simulate various DER penetration levels.

B. Model Reduction

Simulating a large system in real-time is very computationally expensive. Several model reductions have to be done to accommodate the limited computing power of our RTDS system. The first model reduction effort is on secondary cable modeling. In the original LVNTS, the secondary buses are connected by 5–6 parallel cable bundles. There is no magnetic coupling between each bundle. Explicitly modeling these parallel cable bundles would be computationally infeasible. Therefore, we used the pre-built IEEE LVNTS model in the OpenDSS example library to create an equivalent Pi model of each secondary cable section. In addition to cable bundle equivalence, we have to reduce the size of the secondary cable network. In the first step of the reduction, we removed half of the secondary cable network. The remaining network still preserves the original mesh topology. More than that, we noticed that in the original IEEE LVNTS, the secondary cable sections at the outer boundary only have one network transformer connected, while the inner sections have two network transformers connected. In the reduced LVNTS, we kept this network transformer placement pattern. As a consequence of the topology reduction, the total power supply to the remaining network is reduced. This could negatively impact the network voltage profile if the load is kept the same. To mitigate this negative impact, we added seven constant PQ sources at locations that used to have infeed power.

In the second step of the model reduction, we aggregated load buses along a secondary cable section into one equivalent load bus. As depicted in Figure 1, load clusters are color-coded and aggregated to a few load centers. The reduced LVNTS has 98 three-phase buses. Figure 1 also shows the topology of four medium-voltage primary feeders. Each of them is a 2500 feet underground 3-conductor cable section from the substation to the network transformer. For example, in Figure 1, the distance

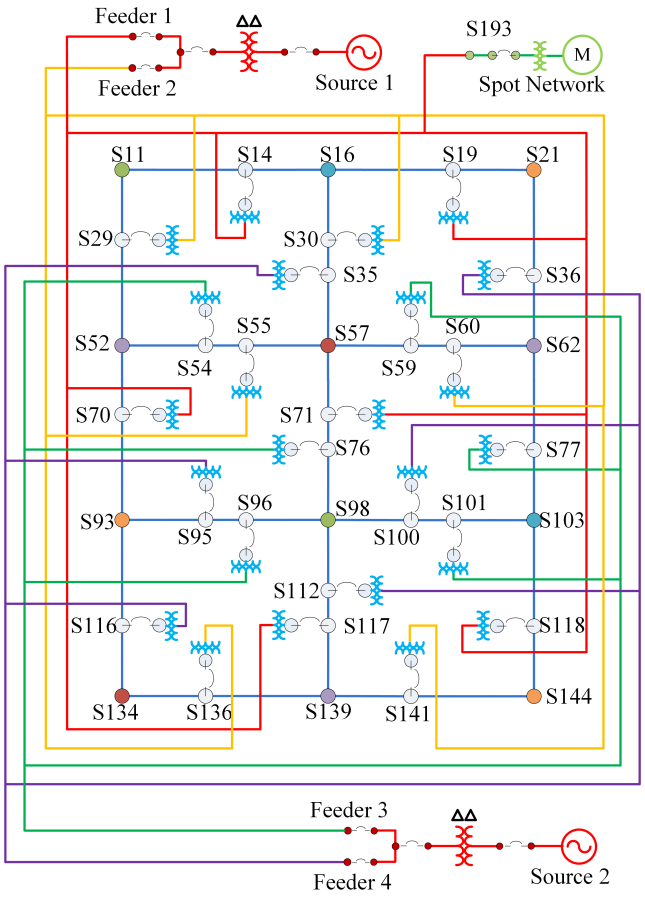

Fig. 1. Reduced 98-bus IEEE LVNTS.

from the head of feeder 1 to secondary bus S14 is 2500 feet. The distance from feeder-1 head to S70 is also 2500 feet.

C. Steady-State Performance Validation

Although it is not possible to have a one-to-one comparison between the original and reduced IEEE LVNTS, it is important to analyze if the reduced model still preserves the electrical characteristics of the original model. To obtain benchmark values, we used the original IEEE LVNTS model in the OpenDSS to calculate all bus voltage, current, and short circuit fault currents at each bus. Note that the OpenDSS model is a phasor-based model, whereas RTDS is an EMT model. Even without any reductions, we don't expect phasor and EMT models to match perfectly. According to the boxplot in Figure 2, the bus voltage in the reduced model is generally higher. Still, both models have buses with voltage as low as 119V. This difference is caused by the load aggregation mentioned above. Due to the aggregation, loads along secondary cables are shifted towards the end and away from network transformers. As a result, the buses near the network transformer will have a higher voltage. In contrast, load buses far from the network transformer will have a lower voltage (constant power load draw more current and causes higher losses). For the same reason, one can observe in Figure 3 that the branch current of

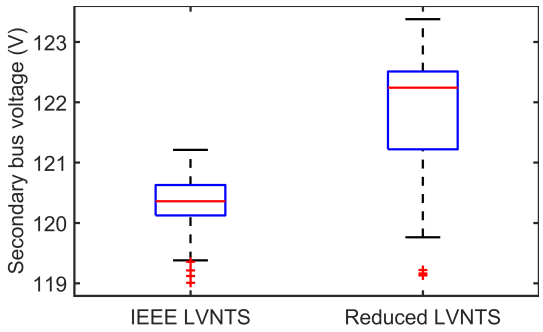

Fig. 2. Boxplot of secondary bus voltages in OpenDSS for the full IEEE LVNTS compared to the reduced LVNTS in RTDS.

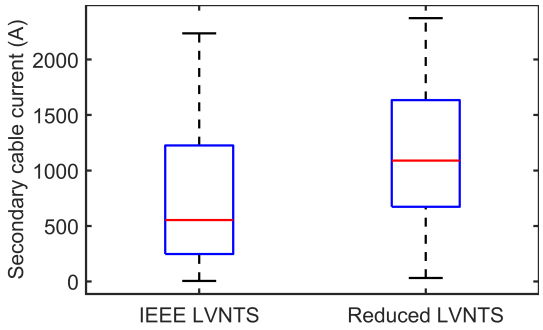

Fig. 3. Boxplot of secondary cable currents in OpenDSS for the full IEEE LVNTS compared to the reduced LVNTS in RTDS.

the reduced model is generally higher than the original model. These deviations are expected, and we believe this will not negatively impact future studies. In conclusion, the reduced model's bus voltage and branch current profiles are reasonably similar to the original model.

D. Short-Circuit Performance Validation

In addition to steady-state performance validation, we strategically selected four secondary bus locations, i.e., S16, S52, S98, and S144, shown in Figure 1, to perform short-circuit validation against the original model in the OpenDSS. Note that fault currents simulated in the RTDS are instantaneous AC values. The root-mean-square (RMS) fault current is calculated for each fault type. For example, during a three-phase fault, a single RMS value is calculated for each simulation time step using three instantaneous fault current values, as shown in Eq. (1).

$$I_{\text{RMS}}(t) = \sqrt{\frac{1}{3} \times (I_{\text{A}}^2(t) + I_{\text{B}}^2(t) + I_{\text{C}}^2(t))} \qquad (1)$$

The RMS of a single-phase fault current, e.g., phase-to-ground and phase-to-phase currents, is measured using the single-phase RMS meter in the RTDS. Its calculation logic is shown in Figure 4. The integrator accumulates the square of the input current value and divides the value by $T = 0.5$ sec. The zero-crossing detector resets the integrator output every half a cycle, i.e., 0.5 sec. This is effectively computing the average of the squared input value. Then, this half-cycle average value is scaled by the measured frequency in Hertz,

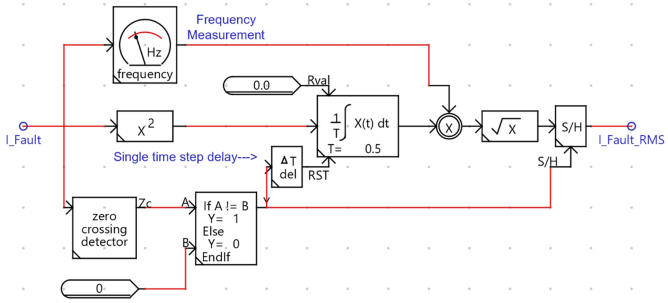

Fig. 4. Single-phase RMS value calculation logic.

TABLE I
FAULT CURRENT COMPARISON: OPENDSS AND RTDS.

Location		S16	S52	S98	S144
1LG	OpenDSS	78976	123304	123389	49269
Fault	RTDS	79904	85418	125831	49477
Current (A)	%Error	1%	31%	2%	0%
Ph-Ph	OpenDSS	101044	158422	157966	64188
Fault	RTDS	99171	103374	155933	63230
Current (A)	%Error	2%	35%	1%	1%
3Phase	OpenDSS	121630	193457	192699	76679
Fault	RTDS	118252	119716	189080	76467
Current (A)	%Error	3%	38%	2%	0%

and a square root is taken on this scaled value to obtain a half-cycle RMS value. Finally, the sample and hold block is used to hold the RMS value for half a cycle while the next half-cycle RMS value is being computed.

Before OpenDSS comparison can be made, we still need to deduce a single RMS value from a time series of RMS values calculated using the above methods. Thus, we took the median value for the first four cycles and used this for the following OpenDSS comparison. The median RMS fault currents for single-phase-to-ground faults, phase-to-phase faults, and three-phase faults are summarized in Table I, from which we can see that all fault currents have good matches with the original model except location S52. This is expected, as the S52 bus is not a boundary bus in the original model. Instead, it is a middle bus with four in-feeds. In the reduced model, due to model reduction, it becomes a boundary bus with only three in-feeds. Therefore, it is not an apple-to-apple comparison, and a deviation from the original model is expected. But one can still qualitatively gauge the accuracy of Location S52 by comparing it with the OpenDSS results of Location S16. Because both S52 and S16 are boundary buses with three in-feeds. One can see that the RTDS S52 fault current values are very similar to the OpenDSS S16 fault current values. In conclusion, the short circuit behavior of the reduced model matches the original model.

IV. Conclusions

This paper is Part 1 of a paper series in which authors performed protection studies in the low-voltage network with high DER penetration. In the Part 1 paper, we categorized the current challenges utilities face into four categories: (1) DER backfeed induced NP misoperation, (2) Voltage profile management, (3) Slow clearing of secondary cable faults, and (4) Microgrid integration. Later HIL protection studies proposed in this paper series are geared toward tackling the first reported challenge. The authors performed a literature survey on the available low-voltage network model and prior protection studies. We found the following two gaps: (1) there are only four publicly available models with low-voltage networks, and only one of them, IEEE LVNTS, is applicable to the study of low-voltage grid networks. (2) The IEEE LVNTS model is only available in phasor-based simulation software. Users need to create EMT models for detailed time-domain protection studies. In this paper, authors modeled a reduced IEEE LVNTS in the RSCAD/RTDS in preparation for proposed real-time HIL protection studies. The steady-state and short-circuit performances of the reduced model are validated against the original IEEE LVNTS model in OpenDSS.

Acknowledgment

This article has been authored by an employee of National Technology & Engineering Solutions of Sandia, LLC under Contract No. DE-NA0003525 with the U.S. Department of Energy (DOE). The employee owns all right, title and interest in and to the article and is solely responsible for its contents. The United States Government retains and the publisher, by accepting the article for publication, acknowledges that the United States Government retains a non-exclusive, paid-up, irrevocable, world-wide license to publish or reproduce the published form of this article or allow others to do so, for United States Government purposes. The DOE will provide public access to these results of federally sponsored research in accordance with the DOE Public Access Plan https://www.energy.gov/downloads/doe-public-access-plan.

References

[1] E. Udren *et al.*, "Roadmap for Advancement of Low-Voltage Secondary Distribution Network Protection," *Sandia National Laboratories*, no. SAND2022–0208, Jan. 2022.

[2] K. P. Schneider *et al.*, "Analytic Considerations and Design Basis for the IEEE Distribution Test Feeders," *IEEE Transactions on Power Systems*, vol. 33, no. 3, pp. 3181–3188, May 2018.

[3] A. Koirala *et al.*, "Non-synthetic European low voltage test system," *International Journal of Electrical Power & Energy Systems*, vol. 118, p. 105712, Jun. 2020.

[4] K. Schneider *et al.*, "IEEE 342-node low voltage networked test system," in *2014 IEEE PES General Meeting | Conference & Exposition*. National Harbor, MD, USA: IEEE, Jul. 2014, pp. 1–5.

[5] M. E. Ropp *et al.*, "Secondary networks and protection: Implications for der and microgrid interconnection," *Sandia National Laboratories*, no. SAND-2020-11209, Nov. 2020.

[6] M. E. Ropp and M. J. Reno, "Influence of Inverter-Based Resources on Microgrid Protection: Part 2: Secondary Networks and Microgrid Protection," *IEEE Power and Energy Magazine*, vol. 19, no. 3, pp. 47–57, May 2021.

[7] P.-C. Chen *et al.*, "Analysis of Voltage Profile Problems Due to the Penetration of Distributed Generation in Low-Voltage Secondary Distribution Networks," *IEEE Transactions on Power Delivery*, vol. 27, no. 4, pp. 2020–2028, Oct. 2012.

[8] P. Mohammadi and S. Mehraeen, "Challenges of PV Integration in Low-Voltage Secondary Networks," *IEEE Transactions on Power Delivery*, vol. 32, no. 1, pp. 525–535, Feb. 2017.

[9] L. J. R. Neiva *et al.*, "Analysis of Power Flow Reversion in Distribution Transformers Due to Medium-Voltage Fault and Distributed Generation in Secondary Networks," *Journal of Control, Automation and Electrical Systems*, vol. 32, no. 6, pp. 1718–1727, Dec. 2021.

[10] Z. Cheng *et al.*, "Low voltage network protection utility workshop — summary and next steps," *Sandia National Laboratories*, no. SAND2022–1406, Feb. 2022.

Zheyuan Cheng received his Ph.D. degree in Electrical Engineering from North Carolina State University in 2020 and his B.Eng. degree in electrical engineering from Nanjing University of Aeronautics and Astronautics in 2015. He has held various roles of increasing responsibility since he joined Quanta Technology in 2020. He holds one US patent and has published over twenty IEEE journal papers and conference proceedings. He is a recipient of the 2021 Best Paper Award from IEEE Industrial Electronics Magazine.

Eric A. Udren has a distinguished 53-year career in the design and application of protective relaying systems, substation control, IEC 61850, wide-area monitoring and control systems, PMU applications, and communications systems. He works with major utilities to develop new substation protection, control, communications, and remedial action scheme designs based on Ethernet, IEC 61850 integration, and synchrophasor techniques. Since 2008 he has served as Executive Advisor with Quanta Technology, LLC of Raleigh, North Carolina, with his office in Pittsburgh, Pennsylvania.

Juergen Holbach Ph.D., Senior Director of Automation and Testing with Quanta Technology, has more than 25 years of experience designing and applying protective relaying. An IEEE member and chairman, he has published over a dozen papers and holds three patents. In 2009, Juergen received the Walter A. Elmore Best Paper Award from the Georgia Tech Relay Conference. Juergen's areas of expertise include automation and protection, transmission protection, real-time digital simulator (RTDS) testing, and International Electrotechnical Commission (IEC) 61850 compliance.

Matthew J. Reno is a Principal Member of Technical Staff in the Electric Power Systems Research Department at Sandia National Laboratories. His research focuses on distribution system modeling and analysis with Big Data and high penetrations of PV by applying cutting edge machine learning algorithms to power system problems. Matthew is also involved with the IEEE Power System Relaying Committee for developing guides and standards for protection of microgrids and systems with high penetrations of inverter-based resources. He received his Ph.D. in electrical engineering from Georgia Institute of Technology.

Michael E. Ropp has over twenty years of experience in research and education in power engineering, power electronics, and photovoltaics. He has authored over eighty technical publications and holds six patents. He is a Senior Member of the IEEE and is active in standards creation, and is a registered Professional Engineer in South Dakota and Hawaii. His primary technical interests are in the planning, design, modeling and simulation, control, dynamics, protection, reliability, diagnosis and event analysis of low-inertia, distributed and inverter-dominated power systems, and he also has a long-standing fascination with electrified transportation. Dr. Ropp is passionate about the education of future electrical engineers and engages in education, mentorship and outreach whenever possible. He does occasionally still get to use his musical skills.

Protection and Control Challenges of Low-Voltage Networks with High Distributed Energy Resources Penetration — Part 2: Impact Assessment and Mitigation Strategy

Zheyuan Cheng, Eric Udren, Juergen Holbach
Quanta Technology
Raleigh, NC, USA
{zcheng, eudren, jholbach}@quanta-technology.com

Matthew J. Reno, Michael E. Ropp
Sandia National Laboratories
Albuquerque, NM, USA
{mjreno, meropp}@sandia.gov

***Abstract*—This is the second part of a two-part paper series. In the Part 1 paper, the authors summarize the utility workshop outcomes and low-voltage network modeling approaches. In this Part 2 paper, we developed and validated an accurate network protector relay model and interfaced a commonly used network protector relay hardware with our real-time simulation system. Hardware-in-the-loop protection studies are performed to assess the impact of distributed energy resources and benchmark a mitigation strategy. Simulation results suggest that the network protector reverse trip and auto-reclose functions are negatively impacted by the high distributed energy resource penetration. To accommodate DER backfeed while remaining secure and reliable for faults on primary feeders, we recommend options for a rate-of-change-based blocking scheme and a protection setting change. Finally, future mitigation ideas and standard revisions are discussed.**

***Index Terms*—Distributed Energy Resources, Hardware-in-the-loop Simulation, Low-voltage Networks, Protective Relaying, Real-Time Digital Simulation.**

I. Introduction

In the Part 1 paper, the authors invited four major U.S. low-voltage network users to a technical workshop to survey the modeling and study needs. In preparation for the proposed real-time hardware-in-the-loop (HIL) protection studies, the authors modeled a reduced 98-bus IEEE low-voltage network test system (LVNTS) in the RSCAD/RTDS. The steady-state and short-circuit performances of the reduced model are validated against the original IEEE LVNTS model in OpenDSS. This Part 2 paper reports the HIL simulation setup, high DER penetration impact assessment, and benchmark results of a promising mitigation solution.

One of the key protection devices in the low-voltage network is the network protector (NP) relay. Its protection functions and hardware specifications are defined in the IEEE C57.12.44-2014 standard [1]. NP relay automatically connects and disconnects a network transformer from a secondary spot or grid network. According to the IEEE C57.12.44-2014 standard, the purpose of the network protector relay is to trip open the protector when there is a net three-phase power flow from the network to the primary (reverse power) and to initiate automatic closure of the protector when there is a potential for a forward flow of power into the low-voltage network. The selected IEEE LVNTS consists of 68 NP relays and protectors. Obviously, it is impractical to acquire 68 relay hardware and interface all of them with the RTDS simulator. A common solution is to only interface with a few hardware devices while using a representative software relay model to simulate the rest of the hardware relays. In this paper, we procured one commonly used hardware NP relay and set it up with an RTDS simulator to perform relay hardware-in-the-loop (HIL) simulation. In terms of the software relay model, the authors are tasked to create an NP relay software simulation model that can accurately reflect the behaviors of the acquired hardware NP relay. Because there are no available NP relay software models in RSCAD/RTDS.

Our literature survey suggests that most DER-related protection studies are performed assuming a typical radial distribution system or a microgrid. The high DER penetration impact on the protection and control of the low-voltage grid network is less understood. A study published in [2] analyzed the voltage profile control issues of a low-voltage grid network in the Manhattan area. In an attempt to determine the maximum amount of DER that the low-voltage grid network can withstand without exhibiting undervoltage and overvoltage problems, the authors performed hundreds of time-domain simulations using the Electromagnetic Transients Program (EMTP) software. In [3], steady-state power flow studies of a low-voltage grid network in the city of New Orleans are conducted to analyze DER impacts on network protection. The authors reported issues related to DER backfeed-induced NP trip and proposed a generalized current differential protection method to protect sections of the primary feeder selectively. In [4], the authors illustrated the DER backfeed-induced NP trip issue using the OpenDSS simulation study of a Brazilian 81-bus test system and the IEEE LVNTS. With respect to prior works, the key contributions of this Part 2 paper are summarized as the following: (1) One commonly used NP relay hardware is interfaced with RTDS to perform HIL protection studies. (2) An accurate NP relay digital twin software simulation model

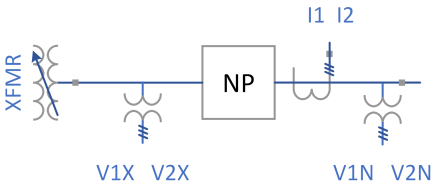

Fig. 1. NP relay conceptual electrical connections.

is developed to be simulated in conjunction with hardware NP relay. (3) A rate-of-change-of-current (ROCOC) based mitigation solution is developed and benchmarked.

The rest of the paper is structured as follows: Section II presents the development and validation of an accurate NP relay software simulation model. Section III discusses the HIL simulation setup and simulation scenarios. Section IV reports the impact assessment results. Section V presents a ROCOC mitigation strategy that can be used in high DER penetration situations. Conclusions are drawn at the end.

II. Network Protector Relay Modeling

The NP relay is typically powered by any two phases of the three-phase transformer or network voltages. Based on the reduced LVNTS modeled in this study, the NP relay is configured with a rated system voltage of 216 V (LL RMS) and a CT ratio of 800. Figure 1 depicts the conceptual electrical connections of an NP relay. The NP relay takes three-phase measurements of the voltage on two sides of the NP (circuit breaker) and the current through the NP. The voltage measured at the secondary side of the network transformer is called transformer voltage VX, and the voltage measured at the network side is called network voltage VN. Symmetrical components are later deduced from the three-phase measurements within the NP relay. For example, $V1X$ and $V2X$ are positive sequence transformer voltage and negative sequence transformer voltage, respectively. Typically, NP relay's protection functions act on positive and negative sequence components instead of per-phase quantities.

A. Model Data Gathering via Probing Tests

In order to develop an accurate NP digital twin model, the authors designed many probing tests to acquire hardware relay behaviors. The first step is to interface the NP relay with the RTDS system. Three-phase voltage and current analog input signals are simulated in RTDS and supplied to the NP relay via power amplifiers, while digital signals transmitted between the relay and RTDS, such as relay trip, close, and breaker status, are interfaced via various digital input/output circuits. The secondary step is to develop HIL simulation models to iterate all possible relay operating conditions and record relay behaviors. The operating quantity of the reverse trip function is the positive sequence current, and the $0°$ reference is the direction of the positive sequence network voltage phasor. Figure 2 presents all the probing test data points of the reverse trip characteristic. One can see that the

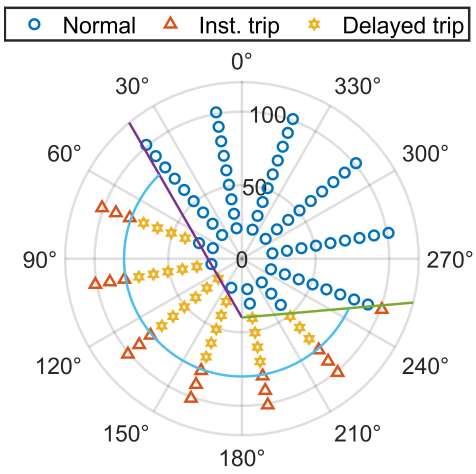

Fig. 2. NP relay reverse trip characteristics. Each data point refers to the positive sequence current magnitude (amps) and angle in reference to the positive sequence network voltage at $0°$.

positive sequence current vector is manipulated to cover all three operation regions: normal operation, delayed trip, and instantaneous trip. This reverse trip characteristic is referred to as the "Watt-Var" trip characteristic. On average, the delayed trip time is 10.085 seconds, and the instantaneous trip time is 119.5 ms. Note that the time delay is set as 10 seconds.

Probing test cases also include scenarios where additional harmonics are introduced to the NP current. The authors injected 5% of the 5^{th}, 7^{th}, and 11^{th} harmonics (a total of 15% harmonics) into three-phase current signals and repeated all the reverse trip probing HIL tests shown in Figure 2. Notably, the reverse trip time behaviors are consistent with the normal condition. No noticeable difference in the trip time is observed. The average instantaneous trip time under 15% harmonics is 121.6 ms, and the average time delayed trip time is 10.087 sec.

The NP relay will automatically reclose when the phasing voltage satisfies pre-defined conditions. The operating quantity of the auto-reclose function is the positive sequence phasing voltage $V1P$. The phasing voltage is the difference between the instantaneous transformer and network voltages. For example, a negative phase angle of the positive sequence phasing voltage, e.g., $V1P\angle -15°$, indicates the network voltage is leading the transformer voltage. Thus, the network will export power when the NP relay closes the breaker. Similar HIL probing tests are designed to manipulate the phasing voltage to cover all three auto-reclose operating regions shown in Figure 3: reclose, no auto-reclose, and no manual reclose regions. Note that the no manual reclose mode not only blocks auto-reclose but also blocks manually issued close breaker commands. On average, the NP relay will issue a close command after the auto-reclose condition exists for 1.1326 seconds. This auto-reclose characteristic is referred to as the "circular close" characteristic.

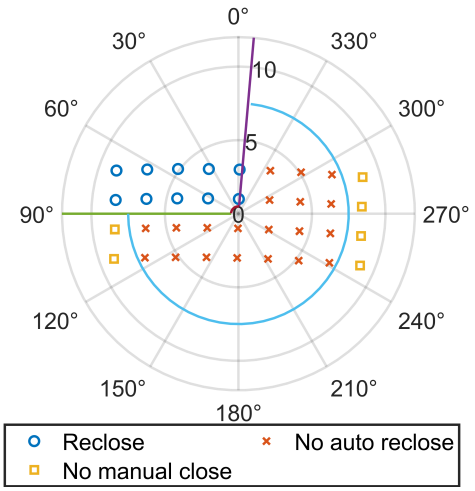

Fig. 3. NP relay auto-reclose characteristics. Each data point refers to the difference between the positive sequence voltages on either side of the NP (volts and angle).

Similar to the previous harmonics injection test for reverse trip function, the authors also injected 5% of the 5^{th}, 7^{th}, and 11^{th} harmonics (a total of 15% harmonics) into the network voltage signals. No noticeable change in auto-reclose behavior is observed.

In addition to reverse trip and auto-reclose functions, the pump protection is manually inspected and verified in the lab. If the NP relay close-trip cycle exceeds 3 cycles in 60 sec, the relay trips NP and locks open. Lockout is reset after 60 min.

Through this HIL probing testing, we accumulated accurate lab-tested data on all necessary relay functions, i.e., reverse trip, auto-reclose, and breaker lockout. This recorded relay behavior data set is then used to develop and validate our in-house NP relay software simulation model.

B. Relay Model Development and Validation

The authors developed an NP relay digital twin model in RSCAD/RTDS based on the relay technical manual and our knowledge about the NP relay operation. The average measured trip/close time values are used to configure the software NP relay model. Probing tests shown in Figure 2 and 3 are repeated with the developed software relay model, and we are able to verify that the simulated trip/close behaviors are consistent with the hardware NP relay.

Dynamic HIL tests are conducted to validate the reverse trip behavior changing positive sequence current. The first test is shown on the left-hand side of Figure 4. The current phasor trajectory is plotted in purple, and the trip state is marked in green. In the first test, the current phasor enters the time-delayed trip zone first and exists before the delay timer reaches 10 sec. This test confirms that the relay will trigger an instantaneous trip as soon as the current vector enters the instantaneous tripping zone despite a pre-existing time-delayed trip timer. The measured instantaneous trip time from the hardware relay is 113.6 ms, and the measured instantaneous

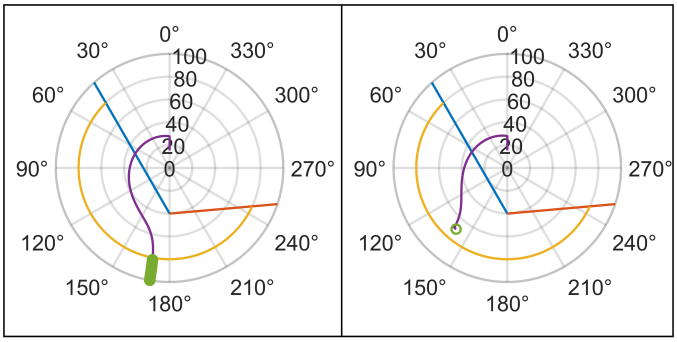

Fig. 4. Reverse trip behavior under changing positive sequence current (shown with a purple trace).

trip time from the software relay model is 119.2 ms. In the second test shown on the right-hand side, the current phasor slid into the delayed trip zone and stayed. This test confirms that the relay will start the delayed trip timer as soon as the current phasor enters the delayed trip zone instead of waiting for it to arrive at a steady state. The measured delayed trip time from the hardware relay is 10.102 sec, and the measured delayed trip time from the software relay model is 10.084 sec.

In Figure 5, additional dynamic HIL tests are conducted to validate the reverse trip behavior when the current phasor transitions between trip zones. In the first test shown on the left, the current phasor trajectory is plotted in purple, and the trip state is marked in green. The current phasor goes in and out of the time-delayed trip zone before the trip command is issued. In this case, the relay will not issue a trip command. In the second test shown on the right, the current phasor enters the time-delayed trip zone the second time after getting out of the zone. In this second dynamic test, we confirm that the relay will reset the delay timer when the current phasor goes out and restart the 10 seconds timer as soon as the current phasor enters the trip zone the second time. Both the hardware relay and the developed software model didn't trip in the first test. During the second test, the measured delayed trip time from the hardware relay is 10.0856 sec, and the measured delayed trip time from the software relay model is 10.084 sec.

The developed digital twin software relay model is verified with the probing test data and validated by additional dynamic HIL tests discussed above. The software model has shown consistent performance compared with the hardware NP relay.

III. HIL Protection Study

This HIL protection study aims to evaluate the performance of the NP relay under high DER penetration. In conventional low-voltage network protection philosophy, the NP is only responsible for clearing primary feeder faults. Faults on the secondary network are to be removed by cable limiters or are to burn clear. We want to examine whether the NP relay will respond correctly to primary, secondary, and network transformer winding faults in this study. As shown in Figure 6, four secondary network fault locations, four primary feeder

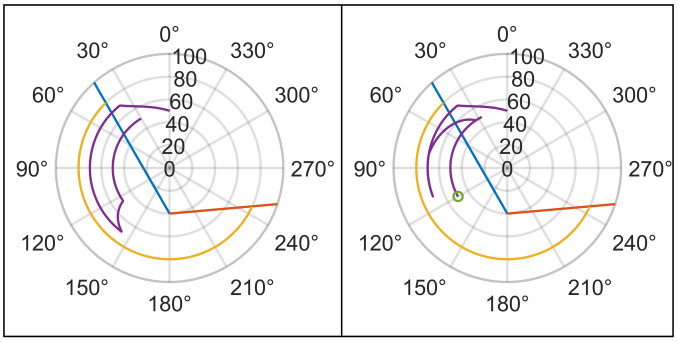

Fig. 5. Reverse trip behavior when the current phasor (shown with a purple trace) transitions between trip zones.

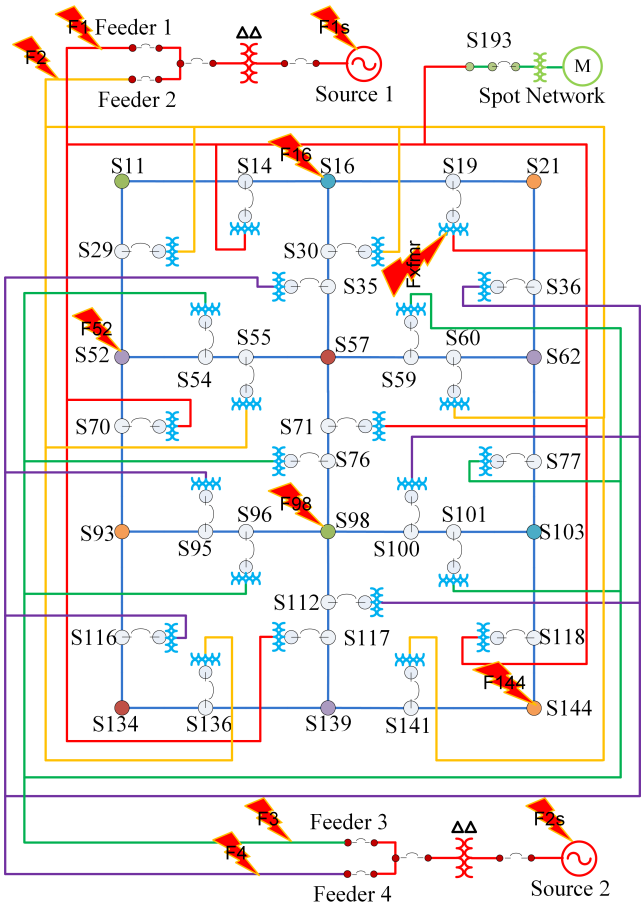

Fig. 6. Reduced 98-bus IEEE LVNTS with fault locations. The low-voltage network is shown in blue with the buses labeled starting with an "S".

fault locations, one network transformer fault location, and two remote 230 kV transmission faults are selected.

A. Simulation Scenarios

Two simulation scenarios are developed for the protection study. The first simulation scenario is designed to investigate the DER backfeed from the secondary network. In this case, we only simulate DER penetration in the secondary network. To achieve various levels of penetration, the DER generation in the low-voltage network will be scaled to 0%, 25%, 50%, and close to 100% of the total load. The nominal inverter output voltage is adjusted to 120 V/208 V, and the rated MVA is adjusted to 1 MVA such that it can be easily scaled to achieve any desired DER penetration level. The inverter model used in the simulation is a very accurate model that is developed and validated using a vendor black-box PSCAD model. This inverter is a neutral-point clamped (NPC) inverter that is equipped with a coupled sequence current control scheme, high/low voltage ride-through control, and over/under voltage protections. Due to RTDS hardware computation limits, it is impossible to add inverter-based DER to every secondary network bus to create high DER penetration cases. Alternatively, the team added three aggregated DER at selected locations, i.e., S11, S62, and S98.

The second simulation scenario aims to evaluate a situation when the low-voltage network is served by a utility source and a large medium-voltage (MV) DER in parallel. The MV DER is expected to maintain electric service during a momentary utility outage and share the network load with the utility source when it is back in service. A grid-forming inverter is required for this simulation scenario. Droop control is identified as a suitable grid-forming scheme for this case, where the inverter operates in parallel with utility sources and supports the low-voltage network when the utility is out of service. We re-purposed a droop-controlled 2-level inverter model from the RTDS example library. The original inverter is a 480V 2MW energy storage inverter. We connected this inverter to the MV bus via a transformer with a scaling factor so that this inverter could be scaled to supply the low-voltage network load.

B. Test Plan

For each simulation scenario, we simulated different fault types in selected locations to properly test the NP relay. The parameters used to change fault characteristics are (1) Fault types: AG, AB, ABG, and ABC, (2) Fault inception angle: 0°, 60°, and 90°, and (3) Fault impedance: Solid fault (10^{-6} Ohm) and high impedance fault (30 Ohm).

Secondary LV network faults are simulated at selected bus locations. The faults are simulated for a fixed period of four cycles. No active fault clearing is modeled or simulated. Primary feeder faults are simulated at 50% of the MV cable. The feeder head breaker opens to clear faults 50 ms after fault inception and auto-recloses 10 seconds after opening. The MV portion of the system is Delta connected (ungrounded). Therefore, a single line-to-ground fault will not create a fault current in individual phases. The feeder head breaker is assumed to be able to detect single line-to-ground faults. Remote transmission faults are simulated by reducing one of the 230 kV utility source voltages to 50% and maintaining 50% voltage for a fixed period (e.g., 100 ms). The transformer winding faults are simulated as a permanent short circuit among three secondary windings. The feeder head breaker is believed to be able to detect the fault and trip at 50 ms.

IV. DER Impacts Assessment

A. Scenario 1: Low-Voltage DER Backfeed

1) Primary Feeder Protection: Primary feeder faults are simulated according to an exhaustive permutation of fault locations and fault configurations mentioned in Section III-B, including up to 100% DER penetration. Testing results suggest that the NP relays connected to the faulted feeder can successfully trip for MV feeder faults. An example MV feeder fault result is presented in Figure 7. In this case, a three-phase fault is simulated for 10 cycles on Feeder #1. All signals from the NP relay connected to Feeder #1 are in red. All signals from the NP relay connected to Feeder #2 are in black. All signals from the NP relay connected to Feeder #3 are in blue. All signals from the NP relay connected to Feeder #4 are in green. According to Figure 7, all four currents flow into the network before the fault. At fault inception, NP relays connected to Feeders #1 and #2 both see reverse current since each has a fault path to the fault on Feeder #1. In contrast, other NP relays see increasing current going into the network, supplying fault from the network side. After 50 ms, the feeder head breaker at Feeder #1 trips and terminates the fault path to the NP relay on Feeder #2, after which NP relays on Feeders #2, #3, and #4 see fault current going into the network supplying the fault from the network side. The NP relay at Feeder #1 eventually correctly trips for this fault. During the process, the ROCOC blocking modules on all four NP relays can pick up the fault current and have sufficient drop-out time delay for the relays to make correct reverse trip decisions. The ROCOC scheme will be discussed in detail in Section V.

However, in high DER penetration cases, we discovered that NP relays near aggregated DER cannot auto-reclose due to the leading network voltage. Its positive sequence phasing voltage resides in the "no auto-reclose" region shown in Figure 3. The leading network voltage will cause a reverse current as soon as the NP relay closes the breaker. Notably, this NP relay will auto-reclose if the user manually shuts down nearby DER sources. Although relaxing the auto-reclose region could potentially solve this problem, this should be done with caution as this may result in unintentional power flow (or power swing) between large MV sources.

2) Secondary Network Cable Fault: None of the NP relays operated in response to secondary cable faults, regardless of DER penetration levels. This test is passed completely.

3) Remote 230 kV Transmission Fault Study: The remote transmission fault was simulated by reducing one of the utility voltages to 0.5 per unit. Since each utility source feeds two feeders, the NP relays connected to these feeders experience voltage drop and reverse current infeed from healthy feeders; DERs trigger reverse trips of all NP relays connected to this faulted utility source. During high DER penetration cases, the NP relays near DER sources experience similar auto-reclose failure caused by a leading network voltage angle, as discussed in Section IV-A1. In conclusion, the tripping behavior is expected, and no new issues are found in this set of test cases.

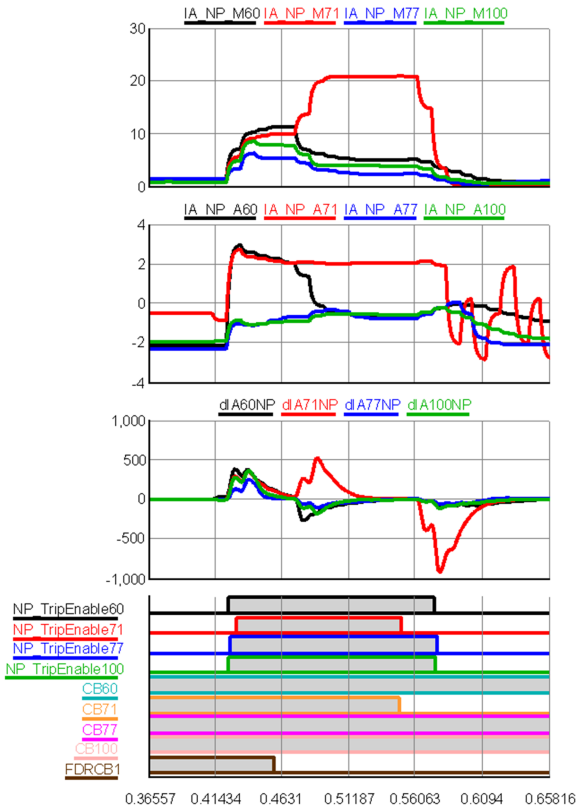

Fig. 7. Example Primary Feeder Fault under 100% DER Penetration.

4) Network Transformer Winding Fault Study: The network transformer winding faults are assumed to be permanent among three secondary windings. To clear this fault from the feeder side, the feeder head breaker trips at 50 ms and stays open as a permanent fault. In this test, the NP relay can successfully trip for reverse current regardless of fault types and DER penetration level.

B. Scenario 2: MV DER Source

We assume that Utility Source #1 serves the low-voltage network with only one feeder while Utility Source #2 is replaced with a large energy storage unit. We simulate one fault on MV Feeder #1 so that Utility Source #1 will be disconnected by the feeder head relay and adjacent network protectors. The energy storage unit will then serve the entire LV network until the restoration of Utility Source #1. This test is focused on DER impacts on MV feeder protection. Therefore, the low-voltage network DER penetration is set at 50% for all cases.

In this scenario, we simulate one fault on MV Feeder #1 so that utility source #1 is disconnected by the feeder head relay and adjacent network protectors. The energy storage unit at source #2 will then serve the entire LV network until the restoration of utility source #1. Test results suggest that the grid-forming inverter MV source modeled in this study can supply sufficient reverse fault current to trigger NP relay tripping on Feeder #1 for all cases, including 30 Ohm resistive

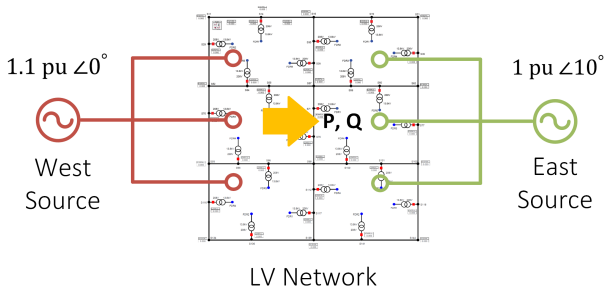

Fig. 8. Unintentional Power Flow between MV Sources.

fault cases. However, we found that the utility source cannot be restored for all MV fault cases when the temporary fault is cleared on MV Feeder #1. For example, we observed the phasing voltage for the Feeder #1 NP relay to be $15V\angle 107°$, which resides in the "no manual reclose" region shown in Figure 3. The lack of synchronization between the energy storage grid-forming inverter and the utility source #1 causes a large angle difference and magnitude difference. This test revealed additional auto-reclose issues that are unique to restoration/black-start situations. When restoring the parallel MV sources, the NP relay will monitor the phasing voltage magnitude and angle and only connect the parallel source when the voltage difference is acceptable. Closing with large phasing voltage magnitude and angle difference will cause a power swing between connected MV sources. In the real-world environment, the restored parallel MV source will likely have a slightly different frequency than the low-voltage network. If the NP relay waits long enough, it could eventually find a suitable reclose moment when the restored parallel MV source converges to the network voltage. This function might be augmented with automatic synchronizer logic, which assesses the rate of slip and initiates closing only for a slip below a safe limit and with close initiation timing to achieve approximately in-phase circuit make. If the grid-forming inverter has a frequency nudge control input, the synchronizer function can adjust DER frequency in small steps until closing is practical.

Another challenge associated with restoring the parallel MV sources is the discrimination of DER backfeed from unintentional power flow between MV sources. If reverse current is allowed at the NP relay to accommodate DER backfeed, it is also possible for MV sources to exchange power across the low-voltage network. As shown in Figure 8, the west MV source has a higher voltage magnitude and a leading voltage angle compared to the east MV source. The west source can drive power flow to the east source after the two are connected. This power flow may be oscillatory or stable, and it is not necessarily dramatic enough for the ROCOC threshold to pick up and release reverse current trip blocking. Therefore, developing a protection scheme that can discriminate between healthy DER backfeed and unintentional power flow between MV sources is critical.

V. Rate-of-Change-of-Current Based Mitigation Solution

Achieving 100% DER penetration with three aggregated DER will cause considerable reverse power flow in nearby network transformers, hence, tripping nearby NP relays. To accommodate the DER backfeed, we developed a ROCOC blocking scheme to differentiate the MV feeder fault current and the DER backfeed current. The logic diagram of the developed ROCOC blocking scheme is presented in Figure 9. The derivatives of the current phasor magnitudes are first calculated and filtered. Through simulation experiments, we settled with a 10-sample (500 μS time step) moving average filter and 0.01-sec time constant filter. A threshold value must be designed to discriminate MV fault and DER backfeed. The underlining assumption is that the reverse fault current has a much higher derivative (or ROCOC) value during fault inception. This threshold value must be sufficiently large to avoid picking up on DER intermittency. Through simulation experiments, 100 kA per second appears to be a good threshold for the reduced IEEE LVNTS system and simulated sources. This threshold can reliably differentiate reverse fault current and DER backfeed current for all simulated faults, including 30 Ohm high resistive fault cases. However, this threshold value should be determined on a case-by-case basis. Because the network apparent impedance (network-side path feeding fault), source impedance, DER penetration level, and fault resistance will all, to some extent, affect the selection of this value. Figure 7 shows an example operation of the developed ROCOC blocking logic. The ROCOC blocking modules on all four NP relays can pick up the fault current and have sufficient drop-out time delay for the relays to make correct reverse trip decisions.

VI. Conclusions

In this Part 2, a HIL protection study is carried out on a reduced IEEE LVNTS with different levels of DER penetrations. The key takeaways of this Part 2 paper are:

- The protection philosophy and relay characteristics specified in IEEE Standard Requirements for Secondary Network Protectors (IEEE Std C57.12.44-2014) need to be revamped to keep up with changing operating conditions.
- To accommodate DER backfeed while remaining secure and reliable for faults on primary feeders, we recommend options for a rate-of-change-based blocking scheme and a protection setting change.
- If reverse current is allowed to accommodate the DER backfeed, it is also possible for MV sources to exchange power across the low-voltage network. Therefore, it is critical to develop a protection scheme that can discriminate reverse fault current, healthy DER backfeed, and unintentional power flow between MV sources.
- This paper presents a methodology for creating an accurate digital twin NP relay model via hardware-in-the-loop data generation and validation. The use of the relay software model significantly reduces the hardware requirements and associated costs.

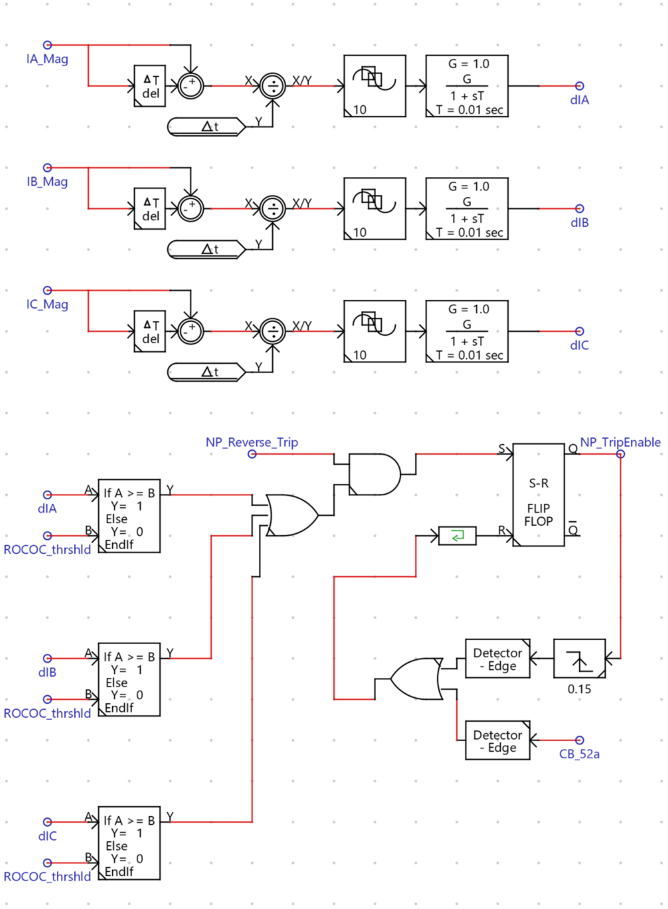

Fig. 9. Example ROCOC Blocking Scheme Logic Implementation.

ACKNOWLEDGMENT

This article has been authored by an employee of National Technology & Engineering Solutions of Sandia, LLC under Contract No. DE-NA0003525 with the U.S. Department of Energy (DOE). The employee owns all right, title and interest in and to the article and is solely responsible for its contents. The United States Government retains and the publisher, by accepting the article for publication, acknowledges that the United States Government retains a non-exclusive, paid-up, irrevocable, world-wide license to publish or reproduce the published form of this article or allow others to do so, for United States Government purposes. The DOE will provide public access to these results of federally sponsored research in accordance with the DOE Public Access Plan https://www.energy.gov/downloads/doe-public-access-plan.

REFERENCES

[1] "IEEE Standard Requirements for Secondary Network Protectors," *IEEE Std C57.12.44-2014 (Revision of IEEE Std C57.12.44-2005)*, Jun. 2014.

[2] P.-C. Chen *et al.*, "Analysis of Voltage Profile Problems Due to the Penetration of Distributed Generation in Low-Voltage Secondary Distribution Networks," *IEEE Transactions on Power Delivery*, vol. 27, no. 4, pp. 2020–2028, Oct. 2012.

[3] P. Mohammadi and S. Mehraeen, "Challenges of PV Integration in Low-Voltage Secondary Networks," *IEEE Transactions on Power Delivery*, vol. 32, no. 1, pp. 525–535, Feb. 2017.

[4] L. J. R. Neiva *et al.*, "Analysis of Power Flow Reversion in Distribution Transformers Due to Medium-Voltage Fault and Distributed Generation in Secondary Networks," *Journal of Control, Automation and Electrical Systems*, vol. 32, no. 6, pp. 1718–1727, Dec. 2021.

Zheyuan Cheng received his Ph.D. degree in Electrical Engineering from North Carolina State University in 2020 and his B.Eng. degree in electrical engineering from Nanjing University of Aeronautics and Astronautics in 2015. He has held various roles of increasing responsibility since he joined Quanta Technology in 2020. He holds one US patent and has published over twenty IEEE journal papers and conference proceedings. He is a recipient of the 2021 Best Paper Award from IEEE Industrial Electronics Magazine.

Eric A. Udren has a distinguished 53-year career in the design and application of protective relaying systems, substation control, IEC 61850, wide-area monitoring and control systems, PMU applications, and communications systems. He works with major utilities to develop new substation protection, control, communications, and remedial action scheme designs based on Ethernet, IEC 61850 integration, and synchrophasor techniques. Since 2008 he has served as Executive Advisor with Quanta Technology, LLC of Raleigh, North Carolina, with his office in Pittsburgh, Pennsylvania.

Juergen Holbach Ph.D., Senior Director of Automation and Testing with Quanta Technology, has more than 25 years of experience designing and applying protective relaying. An IEEE member and chairman, he has published over a dozen papers and holds three patents. In 2009, Juergen received the Walter A. Elmore Best Paper Award from the Georgia Tech Relay Conference. Juergen's areas of expertise include automation and protection, transmission protection, real-time digital simulator (RTDS) testing, and International Electrotechnical Commission (IEC) 61850 compliance.

Matthew J. Reno is a Principal Member of Technical Staff in the Electric Power Systems Research Department at Sandia National Laboratories. His research focuses on distribution system modeling and analysis with Big Data and high penetrations of PV by applying cutting edge machine learning algorithms to power system problems. Matthew is also involved with the IEEE Power System Relaying Committee for developing guides and standards for protection of microgrids and systems with high penetrations of inverter-based resources. He received his Ph.D. in electrical engineering from Georgia Institute of Technology.

Michael E. Ropp has over twenty years of experience in research and education in power engineering, power electronics, and photovoltaics. He has authored over eighty technical publications and holds six patents. He is a Senior Member of the IEEE and is active in standards creation, and is a registered Professional Engineer in South Dakota and Hawaii. His primary technical interests are in the planning, design, modeling and simulation, control, dynamics, protection, reliability, diagnosis and event analysis of low-inertia, distributed and inverter-dominated power systems, and he also has a long-standing fascination with electrified transportation. Dr. Ropp is passionate about the education of future electrical engineers and engages in education, mentorship and outreach whenever possible. He does occasionally still get to use his musical skills.